

Supporting Information

A Series of Lanthanide–quinoxaline-2,3(1H,4H)-dione Complexes Containing 1D Chiral Ln_2O_3 ($\text{Ln} = \text{Eu}, \text{Tb}, \text{Sm}, \text{Dy}$) Chains: Luminescent Properties and Response to Small Molecules

Sadaf ul Hassan,*^{a,b,d} Muhammad Asim Farid^{c,d} and Yingxia Wang*^d

^a University of Management & Technology (UMT), Lahore, 54770, Pakistan

^b COMSATS University Islamabad (CUI), Lahore Campus, Lahore, 54000, Pakistan

^c Department of Chemistry, Division of Science and Technology, University of Education Lahore Pakistan

^d State Key Laboratory of Rare Earth Materials Chemistry and Applications, College of Chemistry and Molecular Engineering, Peking University, Beijing 100871, P. R. China

*Email: yxwang@pku.edu.cn, and sadaf.hassan@umt.edu.pk Tel.: (+8610) 6275 5538 Fax: (+8610) 6275

Table S1 Selected bond lengths [\AA] and angles [$^\circ$] in complex **1**.

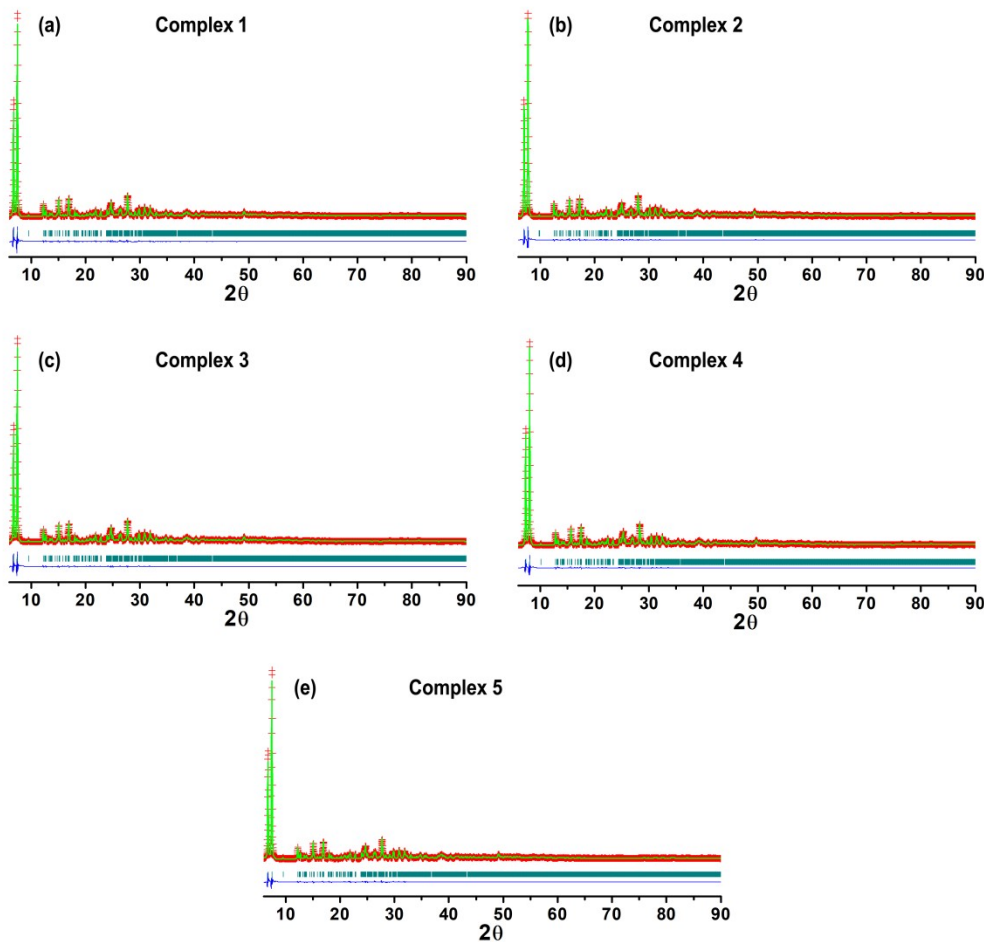
Bond lengths (\AA)			
Eu(1)–O(1)	2.473(7)	Eu(2)–O(1)	2.572(7)
Eu(1)–O(3)	2.452(7)	Eu(2)–O(2)	2.322(7)
Eu(1)–O(4)	2.477(6)	Eu(2)–O(4)	2.439(7)
Eu(1)–O(6) ⁱ	2.443(7)	Eu(2)–O(5)	2.373(7)
Eu(1)–O(7) ^{#ii}	2.354(6)	Eu(2)–O(6)	2.482(6)
Eu(1)–O(7) ^{#iii}	2.376(3)	Eu(2)–O(7) ^{#ii}	2.374(3)
Eu(1)–O(8)	2.424(7)	Eu(2)–O(8) ^{#ii}	2.516(6)
Eu(1)–O(9)	2.406(6)	Eu(2)–O(8) ^{#iii}	2.362(6)
O(1)–C(1)	1.319(3)	O(2)–C(2)	1.308(6)
O(3)–C(9)	1.226(1)	O(4)–C(10)	1.313(6)
O(5)–C(17)	1.264(5)	O(6)–C(18)	1.291(2)
N(1)–C(1)	1.286(2)	N(2)–C(2)	1.302(1)
N(3)–C(9)	1.323(1)	N(4)–C(10)	1.262(1)
N(5)–C(17)	1.310(9)	N(6)–C(18)	1.302(4)
Bond angles			
O(7)–Eu(1)–O(7) ^{#ii}	71.876(2)	O(2)–Eu(2)–O(7) ^{#ii}	94.02(3)
O(7)–Eu(1)–O(8)	72.5(2)	O(8)–Eu(2)–O(8)	74.594(2)
O(9)–Eu(1)–O(8)	83.0(2)	O(8)–Eu(2)–O(5)	130(2)
O(6)–Eu(1)–O(3)	145(1)	O(8)–Eu(2)–O(7) ^{#ii}	127.5(2)
O(7)–Eu(1)–O(6) ⁱ	100.0(2)	O(5)–Eu(2)–O(4)	152.9(2)
O(9)–Eu(1)–O(3)	75.4(3)	O(7) ^{#i} –Eu(2)–O(6)	141.7(2)
O(8)–Eu(1)–O(3)	84.8(2)	O(4)–Eu(2)–O(6)	140.3(2)
O(8)–Eu(1)–O(1)	152.9(2)	O(2)–Eu(2)–O(8)	157.3(2)
Eu(1)–O(7)–Eu(2)	99.3(2)	Eu(1) ^{#iii} –O(6)–Eu(2)	109.3(3)
N(3)–C(9)–C(10)	113.8(1)	O(4)–C(10)–C(9)	111.7(2)

#i -1+x, y, z; #ii -x, 1-y, -z; #iii 1+x, y, z.

Table S2 Hydrogen bonds [Å] and angles [°] found in complex **1**.

D-H···A	D-H (Å)	H···A (Å)	D···A (Å)	D···H···A (°)
Hydrogen bonding interaction between adjacent chiral 1D chains				
N(1)-H(1A)···O(9)	0.88	1.94	2.705	144.2
N(2)-H(2A)···O(10) ^{#i}	0.88	2.02	2.831	153.3
N(4)-H(4A)···O(8) ^{#ii}	0.88	2.10	2.886	147.8
N(5)-H(5A)···O(10)	0.88	2.02	2.789	145.8
N(6)-H(6A)···O(7) ^{#iii}	0.88	1.97	2.781	153.0

#i x+1/2,-y+1/2, z+1/2; #ii x+1, y, z; #iii -x+1,-y+1,-z

**Figure S1.** Rietveld plot of powder X-ray diffraction pattern of the complexes 1-5

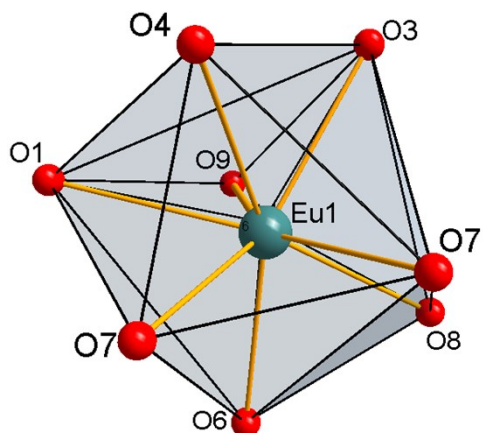


Figure S2. Coordination polyhedron of the Eu1 in complex **1**

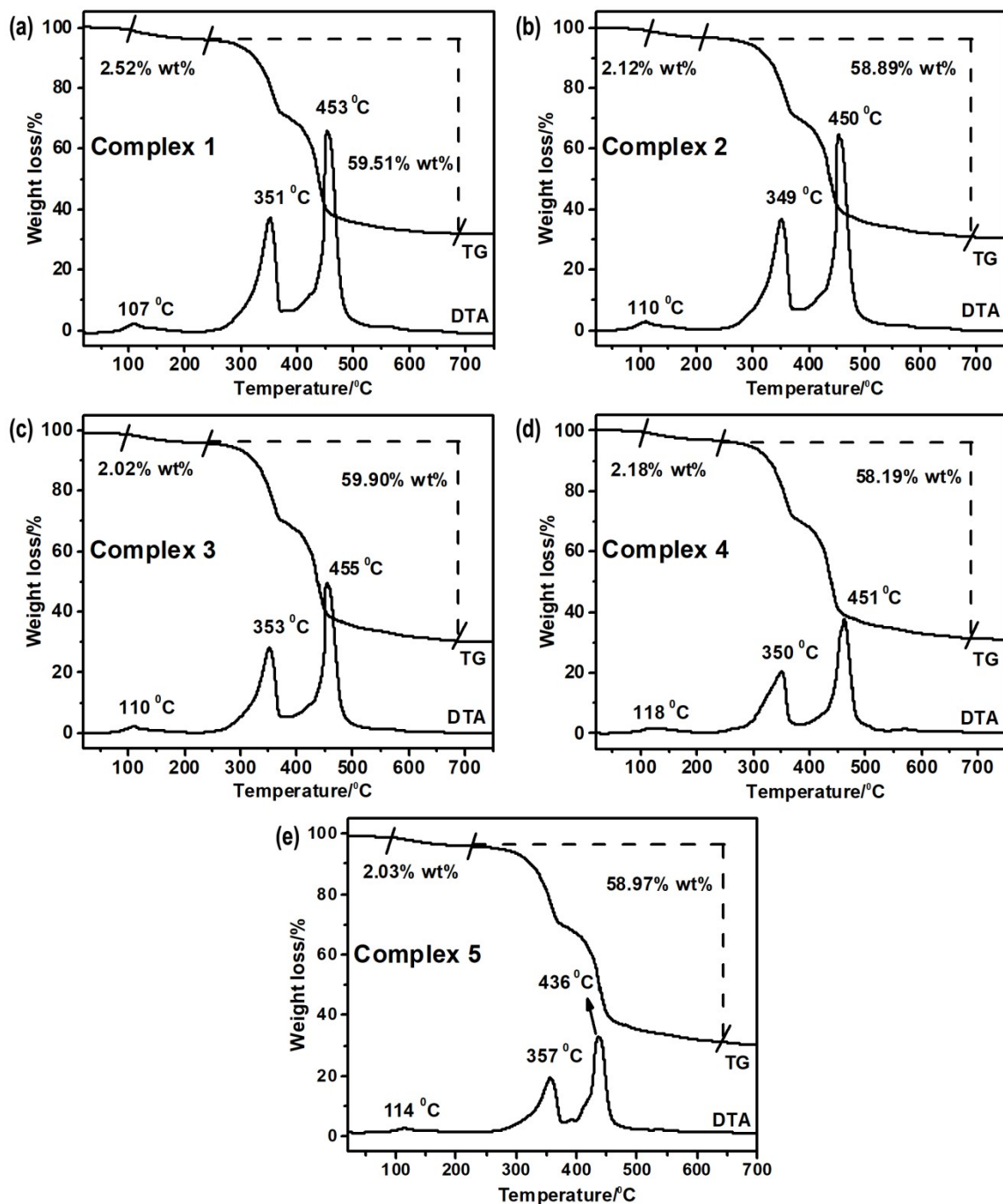


Figure S3. Thermogravimetric analyses (TGA) and differential thermogravimetric analyses (DTA) curves at a heating rate of $10\text{ }^{\circ}\text{C}\cdot\text{min}^{-1}$ under Argon for complexes 1-5.

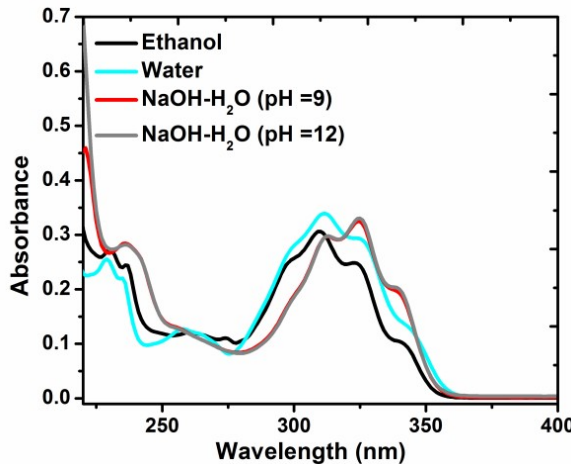


Figure S4. The UV-vis. spectrum of free H₂QXD ligand in ethanol and water (concentration = 1.25×10^{-4} M).

Table S3. Electronic absorption spectral data of ligand in water and ethanol with concentration of 1.25×10^{-4} M.

Solvent	Solvents	Absorptions: λ_{max} (nm), (ϵ , mM ⁻¹ cm ⁻¹)
1	Ethanol	228 (2.19), 236 (1.95), 261 (0.98), 274 (0.91), 298 (2.04), 309 (2.48), 324 (2), 341 (0.8)
2	Water	228 (3.23), 235 (1.76), 257 (1.05), 297 (2.22), 311 (2.74), 326 (2.36), 344 (1.06)
3	NaOH-Water (pH= 9)	236 (2.29), 312 (2.4), 324 (2.61), 340 (1. 62)
4	NaOH-Water (pH= 12)	236 (2.29), 312 (2.4), 324 (2.61), 340 (1. 62)

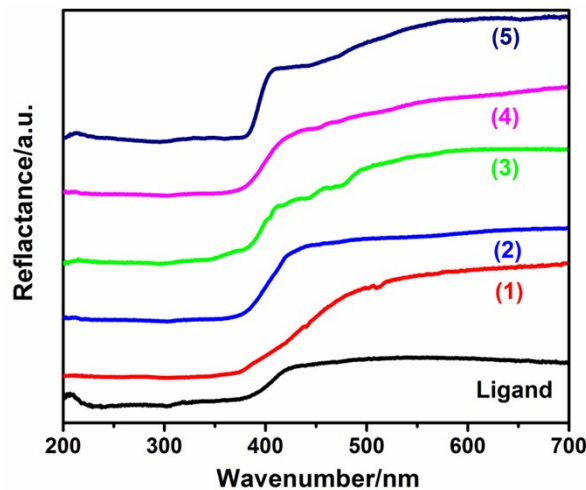


Figure S5. Solid-state diffuse reflectance spectra of the free ligand (black line) and the compounds **1** (red), **2** (blue), **3** (green), **4** (pink) and **5** (navy blue).

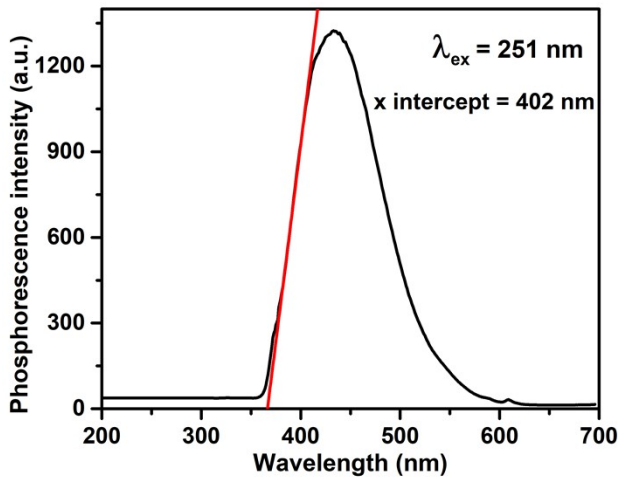


Figure S6. The phosphorescence spectrum of complex **5** at 77 K.

Photo-luminescence properties of complexes **3** and **4**

The excitation bands for complex **3** under the emission of 561 nm show three main peaks at 226, 271 and 333 nm. Under the excitation of 271 nm (the maximum excitation wavelength), the complex **3** shows three emission peaks, at 562, 590 and 670, which may be attributed to ${}^4G_{5/2} \rightarrow {}^6H_{5/2}$, ${}^4G_{5/2} \rightarrow {}^6H_{7/2}$, ${}^4G_{5/2} \rightarrow {}^6H_{9/2}$ transitions respectively (**Figure S7a**).¹ The excitation spectra of complex **4** under the emission of 481 nm exhibit three main peaks at 269 and 346 nm and a characteristic feature corresponding to the metal-centred transition at 367 nm (${}^4M_{9/2} \rightarrow {}^6H_{15/2}$) for the Dy(III) derivatives. The luminescence spectrum shows two apparent emission band at 481 nm (${}^4F_{9/2} \rightarrow {}^6H_{15/2}$) and 574 nm (${}^4F_{9/2} \rightarrow {}^6H_{13/2}$) and a small band at 654 nm (${}^4F_{9/2} \rightarrow {}^6H_{11/2}$) under the excitation of 269 nm (**Figure S7b**).² The complex **4** exhibits typical blue and yellow emission of Dy(III) for ${}^4F_{9/2} \rightarrow {}^6H_n$ ($n = 15/2, 13/2, 11/2$) transitions with little intense band at 481 nm (${}^4F_{9/2} \rightarrow {}^6H_{15/2}$). It is obvious that the intensity of the blue emission, corresponding to the ${}^4F_{9/2} \rightarrow {}^6H_{15/2}$ transition, is a little stronger than that of the yellow one ${}^4F_{9/2} \rightarrow {}^6H_{13/2}$ (**Figure S7b**).

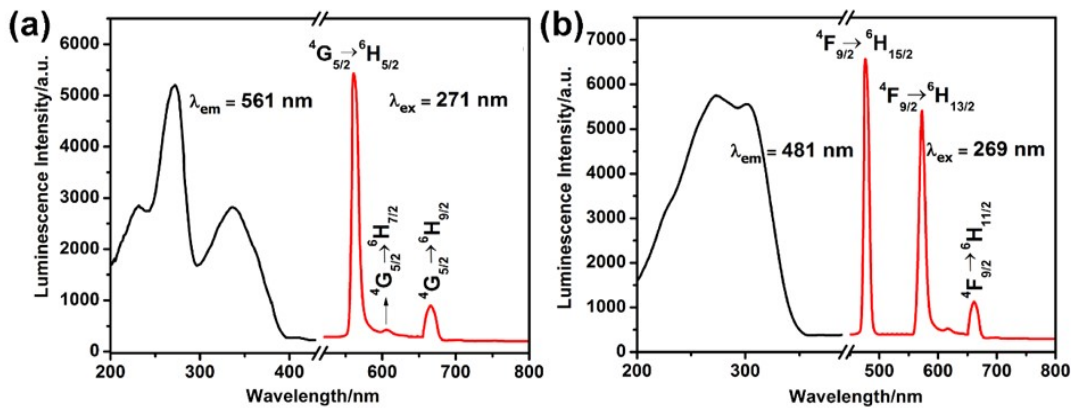


Figure S7. Excitation and emission spectra of: a) $[\text{Sm}_2\text{O}_2(\text{OH})(\text{HQXD})(\text{H}_2\text{QXD})_2] \bullet \text{H}_2\text{O}$ (**3**); b) $[\text{Dy}_2\text{O}_2(\text{OH})(\text{HQXD})(\text{H}_2\text{QXD})_2] \bullet \text{H}_2\text{O}$ (**4**).

Details on Complex 2'

$[\text{Tb}_2\text{O}_2(\text{OH})(\text{HQXD})(\text{H}_2\text{QXD})_2]$ (**2'**): Anal. Calcd. for $\text{C}_{24}\text{H}_{18}\text{N}_6\text{O}_9\text{Tb}_2$ (852 gm): C, 33.82; H, 2.13; N 9.86%. Found: C, 33.80; H, 2.11; N 9.85%. IR (KBr. ν/cm^{-1}): 3002 (w), 2916 (w), 2821 (w), 1630 (s), 1450 (m), 1334 (m), 802 (m), 699 (w), 583 (w) and 518 (w).

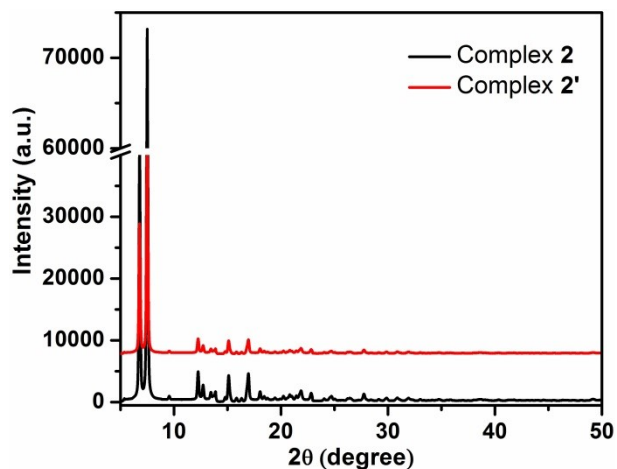


Figure S8. Powder X-ray diffraction profiles of complexes **2** and **2'**.

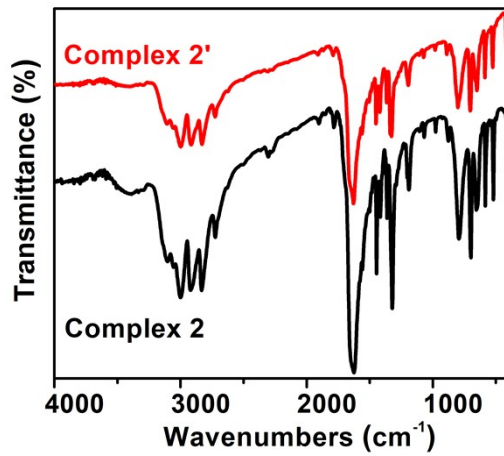


Figure S9. FTIR spectra of complexes **2** and **2'**

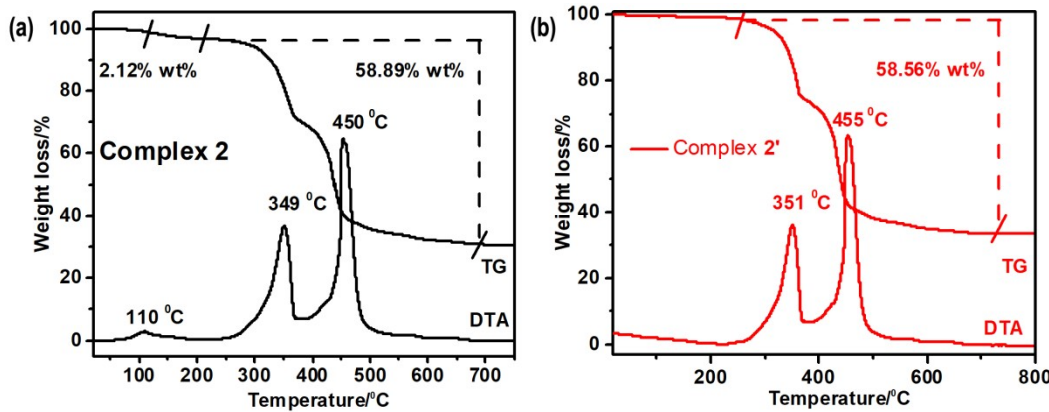


Figure S10 Thermogravimetric analyses (TGA) and differential thermogravimetric analyses (DTA) curves at a heating rate of $10 \text{ }^{\circ}\text{C}\cdot\text{min}^{-1}$ under Argon for complexes (a) **2** and (b) **2'**.

Table S4. The Dielectric constant (k) and normalized Christian Reichard (E_T^N) values of different solvents.

No.	Solvents	E_T^N	Dielectric constant (K)
1	Tert- butanol	0.389	11.2
2	Sec. butanol	0.493	16.6
3	n-butanol	0.536	17.8
4	Iso-propyl alcohol (IPA)	0.546	17.9
5	propanol	0.617	20.1
6	Ethanol (EtOH)	0.654	24.5
7	Methanol (MeOH)	0.762	32.6
8	Water	1.0	80.1
9	DMSO	0.444	46.7
10	DMF	0.386	36.7
11	CHCl ₃	0.259	4.81
12	THF	0.207	7.6

Dielectric constant = K,³ normalized Christian Reichard values = E_T^N

References

1. W. Ahmad, L. Zhang and Y. Zhou, A series of mononuclear lanthanide complexes featuring 3-D supramolecular networks: synthesis, characterization and luminescent properties for sensing guest molecules, *Photochemical & Photobiological Sciences*, 2014, **13**, 660-670.
2. W. Ahmad, L. Zhang and Y. Zhou, 2-D lanthanide–organic complexes constructed from 6, 7-dihydropyrido (2, 3-d) pyridazine-5, 8-dione: synthesis, characterization and photoluminescence for sensing small molecules, *CrystEngComm*, 2014, **16**, 3521-3531.
3. J. A. Riddick, W. B. Bunger and T. K. Sakano, Organic solvents: physical properties and methods of purification, 1986.
4. C. Reichardt, Solvatochromic dyes as solvent polarity indicators, *Chemical reviews*, 1994, **94**, 2319-2358.